Dual Shapiro steps of a phase-slip junction in the presence of a parasitic capacitance

Lisa Arndt,* Ananda Roy, and Fabian Hassler

JARA Institute for Quantum Information, RWTH Aachen University, 52056 Aachen, Germany

(Received 1 March 2018; published 31 July 2018)

Bloch oscillations in a single Josephson junction in the phase-slip regime relate current to frequency. They can be measured by applying a periodic drive to a dc-biased, small Josephson junction. Phase locking between the periodic drive and the Bloch oscillations then gives rise to steps at constant current in the I-V curves, also known as dual Shapiro steps. Unlike conventional Shapiro steps, a measurement of these dual Shapiro steps is impeded by the presence of a parasitic capacitance. This capacitance shunts the junction, resulting in a suppression of the amplitude of the Bloch oscillations. This detrimental effect of the parasitic capacitance can be remedied by an on-chip superinductance. Additionally, we introduce a large off-chip resistance to provide the necessary dissipation. We investigate the resulting system using a set of analytical and numerical methods. In particular, we obtain an explicit analytical expression for the height of dual Shapiro steps as a function of the ratio of the parasitic capacitance to the superinductance. Using this result, we provide a quantitative estimate of the dual Shapiro step height. Our calculations reveal that even in the presence of a parasitic capacitance, it should be possible to observe Bloch oscillations with realistic experimental parameters.

DOI: 10.1103/PhysRevB.98.014525

I. INTRODUCTION

An important goal in quantum metrology is the completion of the metrology triangle between voltage, current, and frequency [1,2]. Bloch oscillations in small Josephson junctions provide the last needed link between current and frequency and thus have the potential to close the metrology triangle [3]. In order to observe these oscillations, a large impedance is needed to reduce the charge fluctuations and reach the Coulomb blockade regime [4,5]. In addition, the Josephson junction needs to be operated as a quantum phase-slip junction, the dual counterpart of the Josephson junction [6–9].

Bloch oscillations can be measured in a quantum phase-slip junction biased with a current I_0 and irradiated with microwaves of frequency ω_0. When I_0 is an integer multiple of $e\omega_0/\pi$, the incident radiation phase locks with the Bloch oscillations in the junction. This leads to dual Shapiro steps in the I-V curve at constant current I_0 [1,3]. The observation of Coulomb blockade is the first prerequisite to observe dual Shapiro steps. It has already been seen in different systems, e.g., nanowires [10,11], Cooper pair transistors [12,13], and single Josephson junctions [14,15]. However, the first attempts to experimentally demonstrate dual Shapiro steps [11,14] did not reveal clear current steps at integer multiples of $e\omega_0/\pi$ in the I-V curves. The experimental difficulties are connected either to the detrimental effects of parasitic capacitances [16] or to the unwanted tunneling of individual electrons [17]. As the latter can be reduced by lowering the temperature, in this work, we concentrate on the effect of the former.

As a remedy for the parasitic capacitances of the biasing lines, a large resistance has to be placed close to the junction, which leads to excessive heating, washing out the dual Shapiro steps [14]. In Ref. [16], it was argued that the complementary requirements (large resistance for good current biasing and small resistance for small heating) are irreconcilable. Furthermore, it was proposed to replace the large resistance by a reactive alternative, a superinductance [18], which reduces the charge fluctuations without introducing heating [13]. The effect of superinductances on dual Shapiro steps was investigated in Refs. [19,20], but without taking into account parasitic capacitances. In this work, we combine an on-chip superinductance, screening the parasitic capacitance, with a large off-chip resistance, dissipating the excess energy. For this setup, we provide analytical results for the height of the dual Shapiro steps and verify our findings using numerical simulations. Our predictions are relevant for the current experimental efforts towards observing dual Shapiro steps. With the recent experimental progress towards building superinductances using Josephson junction arrays [9,13,21–24] or coils [25], we are optimistic of experimental verifications of our theoretical predictions.

This paper is organized as follows. We start by investigating the ideal regime of high impedance, where the characteristic impedance, $Z = \sqrt{L/C_p}$, formed by the superinductance L and the parasitic capacitance C_p is larger than the quantum resistance $R_Q = h/4e^2$. Next, we examine the experimentally more relevant regime $Z \simeq R_Q$, where quantum effects play an important role. Finally, we validate our analytic results by comparing them to numerical simulations.

II. MODEL

The ideal setup for the observation of Bloch oscillations is shown in Fig. 1(a). It is the electrical dual of the conventional Shapiro step experiment [6]. It consists of a voltage source in series with a large resistance and a phase-slip junction. The phase-slip junction can be realized by a (small) Josephson

*lisa.arndt@rwth-aachen.de

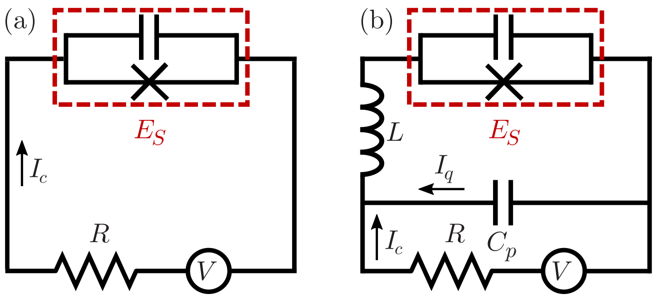

FIG. 1. (a) The ideal setup for the observation of dual Shapiro steps consists of a phase-slip junction E_S in series with a resistance R and an ideal voltage source V. The phase-slip junction is formed by a Josephson junction in parallel to a capacitance. The voltage source V, together with the large resistance R, acts as a current source providing a current I_c. This current can be computed by a direct measurement of the voltage drop across the resistance. (b) In a realistic setup, the phase-slip junction is shunted by an unwanted parasitic off-chip capacitance C_p, causing the part $-I_q$ of the current to flow past the junction. To remedy this unwanted effect, an additional on-chip superinductance L is introduced.

junction with a finite capacitance [1,3,26]. The voltage source drives an incident signal composed of dc and ac components at frequency ω_0 and is given by $V(t) = V_0 + V_{\rm ac}\sin(\omega_0 t)$. Here, we treat the relevant case of $V_{\rm ac} \ll V_0$. In an ideal situation, the large resistance R together with the voltage source constitutes an almost ideal current source with value $V(t)/R$. However, in a realistic situation, an unwanted parasitic capacitance C_p tends to shunt the Josephson junction [Fig. 1(b)]. This could be due to either direct coupling between the leads to and from the junction caused by insufficient separation or indirect coupling between the leads through a common ground plane. As this parasitic capacitance shunts part of the current injected by the source, the Josephson junction will not be perfectly current biased, which results in the Bloch oscillations being washed out.

As a large enough resistance $R \gtrsim R_Q$ causes too much heating, superinductances have been proposed as a reactive alternative in order to suppress fluctuations in the current [9,18,21]. However, as the system is constantly driven, the energy still has to be dissipated at some point. In Ref. [16], the authors proposed to implement the driving as well as the dissipation by a microwave transmission line. In this work, we treat an alternative setup where we combine the idea of the superinductance to protect against parasitic capacitances in the inner current loop with a resistance in series with the voltage source. The key point is that the resistance does not have to be close to the Josephson junction as the superinductance serves to protect against the parasitic capacitance. Rather, the task of the resistance is to turn the voltage source into a current source and to dissipate excess energy so that the system may settle into a stationary state.

The system we propose in order to observe Bloch oscillations is given by Fig. 1(b). In this setup, an inductance L serves to protect against the parasitic capacitance C_p. We denote the current in the outer loop by I_c. The current in this loop is driven by the voltage source, and it is stabilized by the presence of a resistance R. Under the assumption that $R \gg R_Q$, the dynamics of I_c can be treated classically (see also below). Thus, the current I_c can be measured via the voltage drop over the resistance R. On the other hand, the current in the inner loop, denoted by I_q, flows without dissipation and is treated as a quantum-mechanical operator. The current fluctuations are suppressed by the characteristic impedance $Z = \sqrt{L/C_p}$. We need the Josephson junction in the transmon regime with $E_J \gtrsim E_C$ [27]. In this case, the ground-state energy is approximately given by [28]

$$E_S(q) \simeq E_C^{1/4} E_J^{3/4} e^{-(8E_J/E_C)^{1/2}} \cos(\pi q/e), \tag{1}$$

with q being the charge that is accumulated on the capacitor plate. Equivalently, the voltage across the Josephson junction is given by $V_S(q) = V_c \sin(\pi q/e)$, with $eV_c/\pi \simeq E_C^{1/4} E_J^{3/4} e^{-(8E_J/E_C)^{1/2}}$. The capacitance associated with this phase-slip junction is given by $C_S = e/\pi V_c$. In order for Eq. (1) to be a good approximation of the energy stored in the phase-slip junction, the driven system has to stay in the ground state with vanishing Landau-Zener processes [28]. This restricts the drive frequency to $\omega_0 \ll E_J^2/\hbar E_C$, which we take to be true throughout this work.

The step to a quantum description of the problem is performed by introducing the loop charge operators $\hat{Q}_{c[q]} = \int_{-\infty}^{t} dt'\, \hat{I}_{c[q]}(t')$ that denote the charge that has flown in the classical (quantum) loop up to a time t [29]. Kirchhoff's voltage law then demands that

$$R\dot{\hat{Q}}_c = V(t) + \frac{\hat{Q}_q}{C_p}, \tag{2}$$

$$L(\ddot{\hat{Q}}_c + \ddot{\hat{Q}}_q) + V_c \sin[\pi(\hat{Q}_q + \hat{Q}_c)/e] + \frac{\hat{Q}_q}{C_p} = 0. \tag{3}$$

Here, we have included only the noiseless, classical part of the voltage source since we assume that the system is operated at a low enough temperature T, with $k_B T \ll eV_c$. In this case, the thermal noise of the resistance is negligible (for analysis including thermal noise, see Appendix A).

For $R \gg R_Q$, the quantum fluctuations of $\hat{Q}_c$ are suppressed far below $2e$ [5]. As a result, the operator can be simply replaced by its quantum-mechanical expectation value $Q_c = \langle \hat{Q}_c \rangle$. The motion of $\hat{Q}_q$ is given by Eq. (3). This equation describes a nondissipative dynamics of $\hat{Q}_q$ and thus can be described by a Schrödinger equation. The explicit form of the Hamiltonian that leads to the equation of motion for $\hat{Q}_q$ is given by

$$\hat{H} = \frac{\hat{\Phi}_q^2}{2L} + \frac{\hat{Q}_q^2}{2C_p} + L\hat{Q}_q\ddot{Q}_c - \frac{eV_c}{\pi}\cos[\pi(\hat{Q}_q + Q_c)/e], \tag{4}$$

where $\hat{\Phi}_q$ is the canonically conjugate variable of $\hat{Q}_q$ with $[\hat{Q}_q, \hat{\Phi}_q] = i\hbar$ [30]. Note that this Hamiltonian is time dependent, where the time dependence is parametrized by Q_c. Thus, the problem reduces to finding the solution of the time-dependent Schrödinger equation $i\hbar\partial_t\psi(Q_q; Q_c, t) = \hat{H}\psi(Q_q; Q_c, t)$ for the quantum loop charge coupled to the equation of motion

$$R\dot{Q}_c = \langle\psi|\hat{Q}_q|\psi\rangle/C_p + V(t) \tag{5}$$

for the classical loop charge [31]. The dynamics of the circuit are governed by three distinct rates: the plasma frequency of the quantum charge $\omega_q = 1/\sqrt{LC_p}$, the plasma frequency of the classical charge $\omega_c = 1/\sqrt{LC_S}$, and the RC rate $\omega_R = 1/RC_S$ with which the motion is damped. The ratio ω_c/ω_R is the quality factor of the classical charge dynamics and measures the relative importance of the first-order time derivative with respect to the second-order time derivative of Q_c. For $\omega_R > \omega_c$, the system can show hysteretic behavior, which makes it very unfavorable for the accurate observation of dual Shapiro steps. In the following, we will therefore focus on the overdamped regime with $\omega_c \gg \omega_R$.

III. HIGH-IMPEDANCE REGIME

In order to analyze the problem, we first treat the case of a large characteristic impedance $Z \gg R_Q$. In this case, the charge $\hat{Q}_q$ and its fluctuations in the parasitic loop remain small compared to $2e$. This allows us to linearize Eq. (3) and treat $\hat{Q}_q$ classically. Next, we insert the obtained solution for $\hat{Q}_q$ into the equation for the classical loop charge and neglect the second-order derivatives since we are interested in the overdamped regime. This leads to

$$R\dot{Q}_c + \frac{V_c \sin(\pi Q_c/e)}{1 + (C_p/C_S)\cos(\pi Q_c/e)} = V(t). \qquad (6)$$

For vanishing C_p, this reduces to the (dual of the) resistively shunted junction (RSJ) model of the conventional Shapiro steps in the overdamped regime [32]. The resulting voltage steps at fixed dc current I_0 through the outer loop are dual to the conventional Shapiro steps. The position I_0 originates from the phase locking of the external drive frequency ω_0 to the frequency of the Bloch oscillation $I_0\pi/e$. We find that the first step appears at $I_0 = e\omega_0/\pi$ centered around the value $V_0 = V_c\sqrt{1 + (\omega_0/\omega_R)^2}[1 + (3/8)(\omega_R/\omega_0)^2(C_p/C_S)^2]$ of the dc voltage. The step height is given by

$$\Delta V = \frac{V_{\text{ac}}[1 + (1/4)(C_p/C_S)^2]}{\sqrt{1 + (\omega_0/\omega_R)^2}} \qquad (7)$$

to leading order in ω_R/ω_0, C_p/C_S, and V_{ac}/V_c (see Appendix B). The temperature has a negligible effect on the step as long as $k_B T \ll e\Delta V$ (see Appendix A). Note that in this regime the presence of the parasitic capacitance increases the height of the dual Shapiro step.

IV. GROUND-STATE APPROXIMATION

Experimentally more relevant is the regime $Z \simeq R_Q$. In order to obtain analytical results in this regime, we assume the plasma frequency of the quantum charge is large. In particular, we demand that the parasitic capacitance is small enough such that the relations $\omega_q \gg \omega_0$ and $\omega_q \gg eV_c/\hbar \simeq \omega_R R/R_Q$ hold. Under these conditions, the quantum loop charge stays in the ground state of $\hat{H}$ during the course of the evolution, given the system is initially at sufficiently low temperatures with $k_B T \ll \hbar\omega_q$. Specifically, as $\omega_q \gg \omega_0$ and $\hbar\omega_q \gg eV_c$, we can neglect the last two terms in Eq. (4). Then, the ground-state wave function is that of a harmonic oscillator and is given by

$$\psi_0(Q_q, Q_c, t) = \frac{Z^{1/4}}{\pi^{1/4}\hbar^{1/4}} e^{-(Z/2\hbar)Q_q^2 - i\omega_q t/2}. \qquad (8)$$

Using this wave function in order to calculate the expectation value of $\hat{Q}_q/C_p$, the equation of motion of the classical charge reduces to

$$L\ddot{Q}_c + R\dot{Q}_c + e^{-\pi R_Q/2Z} V_c \sin(\pi Q_c/e) = V(t), \qquad (9)$$

valid to lowest order in $eV_c/\hbar\omega_q$ and ω_0/ω_q (see Appendix C). Note that in this equation the sole effect of the parasitic capacitance is to reduce the critical voltage of the phase-slip junction V_c by a factor $e^{-\pi R_Q/2Z}$. This is the main result of our paper. It implies that the effect of the parasitic capacitance is shielded by the inductance as long as the characteristic impedance Z is larger than $\pi R_Q/2 \approx 10\,\text{k}\Omega$. Indeed, we find that in the overdamped regime $\omega_c \gg e^{-\pi R_Q/4Z}\omega_R$, where we can neglect the second-order time derivative, we can again calculate the step height analytically [32]. Assuming that $V_0 > e^{-\pi R_Q/2Z} V_c$ the first step at the current $I_0 = e\omega_0/\pi$ appears at the voltage $V_0 = V_c[e^{-\pi R_Q/Z} + (\omega_0/\omega_R)^2]^{1/2}$. The height (in voltage) of the step at constant current is, on the other hand, given by

$$\Delta V = \frac{V_{\text{ac}}}{\sqrt{1 + e^{\pi R_Q/Z}(\omega_0/\omega_R)^2}}, \qquad (10)$$

valid to first order in $V_{\text{ac}}/e^{-\pi R_Q/2Z} V_c$.

V. NUMERICAL RESULTS

In order to confirm our results, we have performed numerical calculations. First, we solved the coupled system between the Hamiltonian in Eq. (4) and the equation of motion in Eq. (5) numerically. This was done by calculating the time-dependent Schrödinger equation in the basis of the harmonic oscillator using the Crank-Nicolson method, while the classical equation of motion was solved using the backward Euler method. In Fig. 2(a), we compare our numerical results to our analytical solutions from Eq. (7) and Eq. (10). We find that the approximation in the high-impedance regime provides an upper limit to the quantum simulation since the calculation is valid only for $Z \gg R_Q$. The ground-state approximation gives a good, conservative approximation for the size of the step in the quantum simulation, especially for $Z \ll R_Q$. This is due to the fact that the condition for the ground-state approximation $\omega_q \gg eV_c/\hbar \simeq \omega_c\sqrt{Z/R_Q}$ is better fulfilled in this regime.

Second, we solved Eq. (6) numerically using the backward Euler method. The result can be found in Fig. 2(b) together with our analytical result from Eq. (7). As expected, the analytic result works best at small C_p/C_S. Third, we solved Eq. (9) numerically, again using the backward Euler method. In Fig. 2(c), we compare these results to our analytic approximation for the overdamped regime in Eq. (10) for two different values of $\omega_R e^{-\pi R_Q/4Z}/\omega_c$. We find that for $\omega_c \gg e^{-\pi R_Q/4Z}\omega_R$ the numerical calculation agrees very well with the analytical result, as long as the assumption $V_0 > e^{-\pi R_Q/2Z} V_c$ is valid.

In order to better illustrate the dependence of the step size on the parameters, we used the numerical results from the ground-state approximation in Eq. (9) to create the color

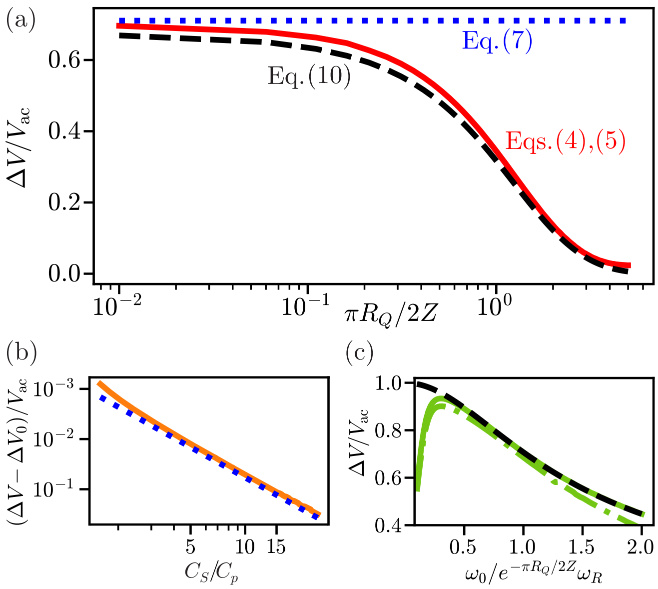

FIG. 2. (a) The height of the first dual Shapiro step as a function of the characteristic impedance Z for $\omega_c/\omega_R = 2, \omega_q/\omega_R = 3, \omega_0/\omega_R = 1.1$, and $V_{ac} = 0.1V_c$. The solid red line shows the result obtained with a numerical calculation of the coupled system of Eqs. (4) and (5). The dotted blue line shows the analytic approximation of the step height in the high-impedance regime $Z \gg R_Q$ in Eq. (7). The dashed black line shows the analytical result of the ground-state approximation in Eq. (10). The ground-state approximation provides a good, conservative approximation for the results of the quantum simulation, especially for $Z \ll R_Q$. (b) Comparison of the analytic approximation of Eq. (7) to the numerical solution of Eq. (6) (solid orange line). The reference step height ΔV_0 corresponds to $C_p = 0$. As expected the approximation works best at large C_S/C_p. (c) Comparison of the analytic result of the ground-state approximation in the overdamped regime [Eq. (10)] to a numerical solution of the classical equation of motion [Eq. (9)]. The solid green line shows the numerical result for $\omega_R e^{-\pi R_Q/4Z}/\omega_c = 0.01$, and the dash-dotted line shows the result for $\omega_R e^{-\pi R_Q/4Z}/\omega_c = 0.5$. The analytical approximation fits the numerical data well, especially for the strongly overdamped regime (solid line).

plot in Fig. 3, which shows the dependence of the step size on all relevant parameters. Here, we can clearly see that the maximum step size can be achieved only in the overdamped regime. For $\omega_c \lesssim e^{-\pi R_Q/4Z}\omega_R$, the step size becomes smaller, and hysteresis begins to occur, making it very unfavorable for a precise measurement of the step position. For $\omega_c > e^{-\pi R_Q/4Z}\omega_R$, the results do not sensitively depend on the parameters used. The optimal step size can be achieved for driving frequencies $\omega_0 \approx 0.5e^{-\pi R_Q/2Z}\omega_R$, with a value ΔV reaching over 80% of the maximal theoretical step size V_{ac}.

VI. EXPERIMENTAL PARAMETERS

Next, we comment on the experimental feasibility of the observation of dual Shapiro steps. Nowadays, it is possible to fabricate Josephson junctions with E_J, $E_C/2\pi\hbar \simeq 10$ GHz [13], which results in critical voltages V_c of the order of 10 μV ($C_S \simeq 5$ fF). In order to avoid Landau-Zener processes, the drive frequency $\omega_0/2\pi$ should remain well below 10 GHz.

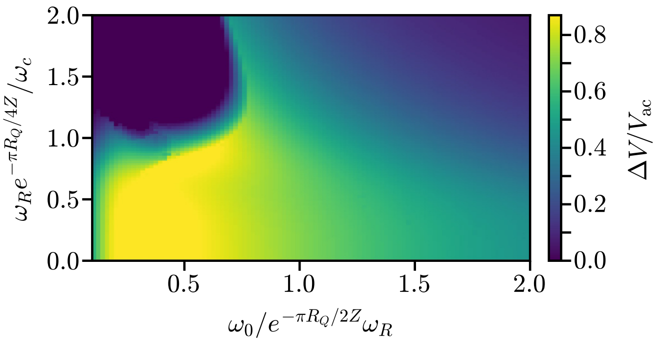

FIG. 3. Size of the first dual Shapiro step in the ground-state approximation as a function of the quality factor and the drive frequency. It was obtained by solving Eq. (9) numerically for $V_{ac} = 0.1e^{-\pi R_Q/2Z}V_c$. It can be seen that the largest steps appear in the overdamped regime $\omega_c \gg e^{-\pi R_Q/4Z}\omega_R$ for a drive frequency $\omega_0 \approx 0.5e^{-\pi R_Q/2Z}\omega_R$.

Therefore, the dual Shapiro steps will appear at currents of the order of nanoamps. In this context, note that a current standard formed by Shapiro steps is readily parallelizable in order to achieve larger values [2]. Modern fabrication techniques allow for on-chip inductances of the order of 500 nH [9,22,25]. For our purposes, we would require a parasitic capacitance of the order of 100 fF in order to obtain an impedance $Z = \sqrt{L/C_p}$ of about 3 kΩ. Given the many groups in different fields working on the fabrication of superinductances, we are confident that this will be reached soon. In addition, sufficiently low temperature as well as effective noise filtering is required to prevent the dual Shapiro steps from being washed out (see Appendix A).

VII. CONCLUSION

In conclusion, we have analyzed the dual Shapiro step height in the presence of a superinductance and a parasitic capacitance. We have described the system by a Schrödinger equation coupled to a classical equation of motion. In the limit $\omega_q \gg \omega_0, eV_c/\hbar$, the quantum system remains in the ground state, and only the classical equation of motion has to be solved. We have provided an analytical expression for the dual Shapiro step height in the overdamped limit $\omega_c \gg e^{-\pi R_Q/4Z}\omega_R$. The leading effect of the parasitic capacitance is a reduction of the critical voltage of the phase-slip junction V_c by a factor of $e^{-\pi R_Q/2Z}$. Thus, the effect of the parasitic off-chip capacitance can be remedied by an on-chip inductance, as long as the characteristic impedance Z is of the order of $\pi R_Q/2 \approx 10$ kΩ. Additionally, we have shown the dependence of the step height on ω_q by deriving an expression for the step height in the limit of high characteristic impedance. Finally, we have performed numerical simulations to validate the analytical results. Throughout this work, we have chosen to neglect the effects of thermal noise of the resistance and the influence of the stray capacitance parallel to the inductance. This is because thermal effects can be made small by working at low temperature and the stray capacitance is usually much smaller than the parasitic capacitance. A detailed analysis of these effects is left for the future.

ACKNOWLEDGMENTS

We acknowledge fruitful discussions with M. H. Devoret, J. Fink, M. Peruzzo, and I. M. Pop. A.R. acknowledges the support of the Alexander von Humboldt Foundation.

APPENDIX A: INFLUENCE OF THERMAL NOISE

Throughout the paper, we assume that the temperature is sufficiently low to keep the dual Shapiro steps from being washed out. Here, we want to comment on the influence of noise on the step height. First, we will discuss the influence of the thermal noise of the resistance. There have been extensive studies on the influence of thermal, white noise for the RSJ model of the conventional Shapiro step experiment [32], which can be easily transferred to the problem of dual Shapiro steps. As an effective noise parameter, we obtain

$$\gamma = 2\pi \frac{k_B T}{e\Delta V}\frac{R}{R_d(V_0)}\left(1+\frac{V_c^2}{2V_0^2}\right), \quad \text{(A1)}$$

with the differential resistance $R_d(V_0) = RV_c\sqrt{(V_0/V_c)^2-1}/V_0$ and V_0 being the dc voltage around which the first dual Shapiro step is centered. The washing out of the step takes place at $\gamma \sim 1$, which leads to a suppression of steps smaller than $\Delta V \simeq V_c$ ($V_c \simeq 10\,\mu$V) at a temperature of $T \simeq 20$ mK. This would suggest that for a resistor at $T \simeq 100$ mK even the measurement of Coulomb blockade is not possible. However, effective filtering methods can be employed to significantly lower the thermal noise of resistors at higher temperatures. This has been repeatedly demonstrated in Coulomb blockade measurements [12–15].

Next, we discuss the influence of charge fluctuations in the LC circuit composed of the parasitic capacitance C_p and the superinductance L (see Appendix C). If we include thermal excitation of higher energy levels in our ground-state approximation, Eq. (C2) has to be rewritten in terms of the trace with the density operator $\hat{\rho}$,

$$\mathrm{Tr}\{\hat{\rho}\sin[\pi(\hat{Q}_q+Q_c)/e]\} = e^{-\pi R_Q(1+2\bar{n})/2Z}\sin(\pi Q_c/e), \quad \text{(A2)}$$

where $\bar{n} = [\exp(\hbar\omega_q/k_B T)-1]^{-1}$ is the average number of photons in the LC resonator given by the Bose-Einstein statistic. For a realistic resonance frequency of the order of $\omega_q \simeq 5$ GHz and a temperature of $T \simeq 20$ mK, we obtain $\bar{n} \simeq 0.1$. The influence of charge fluctuations in the LC resonator is thus negligible.

APPENDIX B: ANALYTICAL CALCULATION IN THE HIGH-IMPEDANCE REGIME

We analyze the system in the regime of large characteristic impedance $Z \gg R_Q$. In this case, the charge $\hat{Q}_q$ and its fluctuations in the parasitic loop remain small compared to $2e$. This allows us to linearize Eq. (3) and treat $\hat{Q}_q$ classically. Next, we insert the obtained solution for $\hat{Q}_q$ into the equation for the classical loop charge. In the overdamped regime, $\omega_c \gg \omega_R$, we can then additionally neglect the second-order time derivatives, which leads to Eq. (6). If we now expand this equation up to second order in small C_p/C_S, we obtain

$$\dot{N}/\omega_R + \sin(N) - (C_p/2C_S)\sin(2N) + (C_p/2C_S)^2[\sin(N)+\sin(3N)] = v(t), \quad \text{(B1)}$$

where $v(t) = V(t)/V_c$ is the normalized voltage and $N = \pi Q_c/e$ is the normalized charge in the classical loop. For vanishing C_p, this again reduces to the (dual of the) RSJ model of the conventional Shapiro steps in the overdamped regime [32]

$$\dot{N}/\omega_R + \sin(N) = v(t). \quad \text{(B2)}$$

For the RSJ model, we can calculate the step height analytically to leading order in V_{ac}/V_0 [32].

We start by calculating the solution to Eq. (B2) without an ac drive, $v(t) = v_0$, and obtain for $v_0 > 1$

$$N_{\mathrm{DC}} = 2\arctan\left\{\frac{i_0}{v_0-1}\tan\left[\frac{\omega_R i_0(t-t_0)+\frac{\pi}{2}}{2}\right]\right\} - \frac{\pi}{2}, \quad \text{(B3)}$$

where $i_0 = I_0 R/V_c = \sqrt{v_0^2-1}$ is the normalized average current running through the classical loop. The initial condition can always be fulfilled by choosing an appropriate t_0.

Now, we will include a small ac drive in addition to the dc bias and expand the solution to Eq. (B2) in a Taylor series $N = N_{\mathrm{DC}} + v_{\mathrm{ac}}N_{\mathrm{AC}}$. We also need to take into account that the ac drive can change the average voltage. Therefore, we will formally expand the dc bias in a Taylor series $v(t) = v_0 + v_{\mathrm{ac}}[v_s + \sin(\omega_0 t)]$, too. Here, v_s acts as the additional influence on the average voltage due to the ac drive. If we insert both expansions into Eq. (B2), we obtain a differential equation for N_{AC},

$$\dot{N}_{\mathrm{AC}}/\omega_R + \cos(N_{\mathrm{DC}})N_{\mathrm{AC}} = v_s + \sin(\omega_0 t). \quad \text{(B4)}$$

This equation does not need to be solved in order to obtain the dual Shapiro step size. Instead, we will specifically consider the first step where $\omega_0 = \omega_R i_0$. At the step, the average current has to remain constant $\overline{\dot{N}_{\mathrm{AC}}} = 0$. Using Eq. (B4), this restraint can be rewritten to obtain

$$\overline{[v_s + \sin(\omega_R i_0 t)]/\dot{N}_{\mathrm{DC}}} = 0, \quad \text{(B5)}$$

which depends only on the solution without an ac drive that we already obtained in Eq. (B3). As a final result, we thus obtain an equation for v_s,

$$v_s = -\cos(\omega_R i_0 t_0)/2v_0. \quad \text{(B6)}$$

We find that depending on the phase shift t_0 between the Bloch oscillations and the ac drive, v_s and thus the position on the voltage step vary. This results in a maximum size of the first step $\Delta V_0 = V_{\mathrm{ac}}/v_0$, which coincides with Eq. (7) in the limit $C_p \to 0$.

Next, we want to obtain the step size for finite C_p up to second order in small C_p/C_S. Like for the previous calculation, we first need to find a solution to Eq. (B1) in the case without an ac drive. We will therefore make the ansatz $N_{\mathrm{DC}} = N_{\mathrm{DC}}^{(0)} + (C_p/2C_S)N_{\mathrm{DC}}^{(1)} + (C_p/2C_S)^2 N_{\mathrm{DC}}^{(2)}$, and we also expand the dc drive $v = v_0 + (C_p/2C_S)v_1 + (C_p/2C_S)^2 v_2$ in the same way. The result for $N_{\mathrm{DC}}^{(0)}$ can be found in Eq. (B3). In order to obtain the higher-order contributions, we separate Eq. (B1) and arrive at the expression

$$\int dN_{\rm DC}\{v_0-\sin(N_{\rm DC})+(C_p/2C_S)[v_1+\sin(2N_{\rm DC})] + (C_p/2C_S)^2[v_2-\sin(N_{\rm DC})-\sin(3N_{\rm DC})]\}^{-1} = \omega_R(t-t_0). \tag{B7}$$

Now, we expand the integrand up to second order in small C_p/C_S and perform the resulting integrals. Then, we can insert the expansion for N_{DC} and sort the expression in orders of C_p/C_S. While the zeroth-order term will lead to Eq. (B3), solving the higher-order terms in succession results in analytical expressions for $N_{\rm DC}^{(1)}$ and $N_{\rm DC}^{(2)}$. Since both expressions are quite involved, we will refrain from writing them down here. As the next step, we will choose v_1 and v_2 in such a way that $\overline{\dot{N}_{\rm DC}^{(1)}}, \overline{\dot{N}_{\rm DC}^{(2)}} = 0$. In this way, the average current will depend on only the zeroth-order contribution, and our former relation $i_0 = I_0R/V_c = \sqrt{v_0^2-1}$ will thus remain valid throughout the calculation. If we apply the condition to our analytical results, we obtain

$$v_1(v_0) = 0, \tag{B8}$$

$$v_2(v_0) = 6v_0 - 4v_0^3 + 4\big(v_0^2-1\big)^{3/2}. \tag{B9}$$

The first step at $I_0 = e\omega_0/\pi$ thus appears close to the value $V_0 = V_c[v_0 + (C_p/2C_S)^2 v_2(v_0)]$, with $v_0 = \sqrt{1+\omega_0^2/\omega_R^2}$. In order to calculate the step height, we need to use Eq. (B5) again, which remains valid in the case $C_p \neq 0$. Going through the same steps as before, we finally obtain the height of the first step,

$$\Delta V = \frac{V_{\rm ac}}{v_0}\left\{1+\left(\frac{C_p}{2C_S}\right)^2\left[1+\frac{29}{96v_0^2}+O\left(\frac{1}{v_0^3}\right)\right]\right\}, \tag{B10}$$

valid to leading order in $V_{\rm ac}/V_c$ and C_p/C_S.

APPENDIX C: DERIVATION OF THE GROUND-STATE APPROXIMATION

In the regime $R \gg R_Q$, the system can be described by the Hamiltonian in Eq. (4) coupled to the equation of motion in Eq. (5). Our calculation will be done in the overdamped regime with $\omega_c \gg \omega_R$. In order to obtain an analytical result, we will assume the quantum plasma frequency is large enough that the relations $\omega_q \gg \omega_0$ and $\omega_q \gg eV_c/\hbar$ are fulfilled. In this case, the last two terms in Eq. (4) can be neglected, and the system will remain in the ground state of the harmonic oscillator with the ground-state wave function given by Eq. (8). Next, we need to approximate the expectation value of $\hat{Q}_q/C_p$. Since we assume C_p is a small parameter in our expansion, we cannot simply take the expectation value of $\hat{Q}_q$ in the ground state. Instead, we express $\hat{Q}_q/C_p$ in terms of the commutator $[\hat{H},\hat{\Phi}_q]$,

$$\hat{Q}_q/C_p = [\hat{H},\hat{\Phi}_q]/i\hbar - L\ddot{Q}_c - V_c\sin(\pi[\hat{Q}_q+Q_c]/e). \tag{C1}$$

Within our approximation, the expectation value of the commutator is zero, and we therefore have to calculate only the expectation value of

$$\langle\psi_0|\sin(\pi[\hat{Q}_q+Q_c]/e)|\psi_0\rangle = e^{-\pi R_Q/2Z}\sin(\pi Q_c/e). \tag{C2}$$

If we insert both results in Eq. (5), we obtain a simplified equation of motion for the classical charge, which can be found in Eq. (9).

[1] K. K. Likharev and A. B. Zorin, J. Low Temp. Phys. **59**, 347 (1985).
[2] J. P. Pekola, O.-P. Saira, V. F. Maisi, A. Kemppinen, M. Möttönen, Y. A. Pashkin, and D. V. Averin, Rev. Mod. Phys. **85**, 1421 (2013).
[3] D. V. Averin, A. B. Zorin, and K. K. Likharev, Zh. Eksp. Teor. Fiz. **88**, 692 (1985) [Sov. Phys. JETP **61**, 407 (1985)].
[4] A. Schmid, Phys. Rev. Lett. **51**, 1506 (1983).
[5] *Single Charge Tunneling*, edited by H. Grabert and M. H. Devoret, NATO Advanced Studies Institute, Series B: Physics Vol. 294 (Plenum, New York, 1992).
[6] J. E. Mooij and Yu. V. Nazarov, Nat. Phys. **2**, 169 (2006).
[7] I. M. Pop, I. Protopopov, F. Lecocq, Z. Peng, B. Pannetier, O. Buisson, and W. Guichard, Nat. Phys. **6**, 589 (2010).
[8] O. V. Astafiev, L. B. Ioffe, S. Kafanov, Y. A. Pashkin, K. Y. Arutyunov, D. Shahar, O. Cohen, and J. S. Tsai, Nature (London) **484**, 355 (2012).
[9] N. A. Masluk, I. M. Pop, A. Kamal, Z. K. Minev, and M. H. Devoret, Phys. Rev. Lett. **109**, 137002 (2012).
[10] T. T. Hongisto and A. B. Zorin, Phys. Rev. Lett. **108**, 097001 (2012).
[11] J. S. Lehtinen, K. Zakharov, and K. Y. Arutyunov, Phys. Rev. Lett. **109**, 187001 (2012).
[12] D. B. Haviland, Y. Harada, P. Delsing, C. D. Chen, and T. Claeson, Phys. Rev. Lett. **73**, 1541 (1994).
[13] S. Corlevi, W. Guichard, F. W. J. Hekking, and D. B. Haviland, Phys. Rev. B **74**, 224505 (2006).
[14] L. S. Kuzmin and D. B. Haviland, Phys. Rev. Lett. **67**, 2890 (1991).
[15] D. B. Haviland, L. S. Kuzmin, P. Delsing, and T. Claeson, Europhys. Lett. **16**, 103 (1991).
[16] V. E. Manucharyan, Ph.D. thesis, Yale University, 2012, Chap. 5.4.
[17] H. Vora, R. L. Kautz, S. W. Nam, and J. Aumentado, Phys. Rev. B **96**, 054505 (2017).
[18] J. Koch, V. Manucharyan, M. H. Devoret, and L. I. Glazman, Phys. Rev. Lett. **103**, 217004 (2009).
[19] W. Guichard and F. W. J. Hekking, Phys. Rev. B **81**, 064508 (2010).
[20] A. Di Marco, F. W. J. Hekking, and G. Rastelli, Phys. Rev. B **91**, 184512 (2015).
[21] V. E. Manucharyan, J. Koch, L. Glazman, and M. Devoret, Science **326**, 113 (2009).

[22] M. T. Bell, I. A. Sadovskyy, L. B. Ioffe, A. Y. Kitaev, and M. E. Gershenson, Phys. Rev. Lett. **109**, 137003 (2012).
[23] C. Altimiras, O. Parlavecchio, P. Joyez, D. Vion, P. Roche, D. Esteve, and F. Portier, Appl. Phys. Lett. **103**, 212601 (2013).
[24] T. Weißl, G. Rastelli, I. Matei, I. M. Pop, O. Buisson, F. W. J. Hekking, and W. Guichard, Phys. Rev. B **91**, 014507 (2015).
[25] J. M. Fink, M. Kalaee, A. Pitanti, R. Norte, L. Heinzle, M. Davanco, K. Srinivasan, and O. Painter, Nat. Commun. **7**, 12396 (2016).
[26] A. B. Zorin, Phys. Rev. Lett. **96**, 167001 (2006).
[27] A. A. Houck, J. Koch, M. H. Devoret, S. M. Girvin, and R. J. Schoelkopf, Quantum Inf. Process. **8**, 105 (2009).
[28] J. Koch, T. M. Yu, J. Gambetta, A. A. Houck, D. I. Schuster, J. Majer, A. Blais, M. H. Devoret, S. M. Girvin, and R. J. Schoelkopf, Phys. Rev. A **76**, 042319 (2007).
[29] J. Ulrich and F. Hassler, Phys. Rev. B **94**, 094505 (2016).
[30] Note that in the loop charge description, charge acts as position [29].
[31] This is in contrast to the calculation of conventional Shapiro steps where the dynamics is described by only one classical degree of freedom [32].
[32] K. K. Likharev, *Dynamics of Josephson Junctions and Circuits* (Gordon and Breach, New York, 1986).